Polymorphic tandem DNA repeats activate the human telomerase reverse transcriptase gene

Tao Xu[a,b,1], De Cheng[a,1], Yuanjun Zhao[c], Jinglong Zhang[a], Xiaolu Zhu[a], Fan Zhang[a], Gang Chen[a], Yang Wang[b], Xiufeng Yan[b,d], Gavin P. Robertson[e,f,g,h], Shobhan Gaddameedhi[i], Philip Lazarus[a], Shuwen Wang[a], and Jiyue Zhu[a,2]

[a]College of Pharmacy and Pharmaceutical Sciences, Washington State University, Spokane, WA 99210; [b]College of Life Science, Northeast Forestry University, Harbin 150040, China; [c]Department of Cellular and Molecular Physiology, Pennsylvania State University College of Medicine, Hershey, PA 17033; [d]College of Life and Environmental Science, Wenzhou University, Chashan University Town, Wenzhou 325035, China; [e]Department of Pharmacology, Pennsylvania State University College of Medicine, Hershey, PA 17033; [f]Department of Pathology, Pennsylvania State University College of Medicine, Hershey, PA 17033; [g]Department of Dermatology, Pennsylvania State University College of Medicine, Hershey, PA 17033; [h]Department of Surgery, Pennsylvania State University College of Medicine, Hershey, PA 17033; and [i]Center for Human Health and the Environment, Department of Biological Sciences, North Carolina State University, Raleigh, NC 27606

Edited by Jue Lin, University of California, San Francisco, CA, and accepted by Editorial Board Member Kiyoshi Mizuuchi April 3, 2021 (received for review September 9, 2020)

Multiple independent sequence variants of the *hTERT* locus have been associated with telomere length and cancer risks in genome-wide association studies. Here, we identified an intronic variable number tandem repeat, VNTR2-1, as an enhancer-like element, which activated hTERT transcription in a cell in a chromatin-dependent manner. VNTR2-1, consisting of 42-bp repeats with an array of enhancer boxes, cooperated with the proximal promoter in the regulation of hTERT transcription by basic helix–loop–helix transcription factors and maintained hTERT expression during embryonic stem-cell differentiation. Genomic deletion of VNTR2-1 in MelJuSo melanoma cells markedly reduced hTERT transcription, leading to telomere shortening, cellular senescence, and impairment of xenograft tumor growth. Interestingly, VNTR2-1 lengths varied widely in human populations; *hTERT* alleles with shorter VNTR2-1 were underrepresented in African American centenarians, indicating its role in human aging. Therefore, this polymorphic element is likely a missing link in the telomerase regulatory network and a molecular basis for genetic diversities of telomere homeostasis and age-related disease susceptibilities.

telomere and telomerase | *hTERT* gene | repetitive DNA elements | polymorphism and genetic diversities | human longevity

Telomeres are ends of chromosomes and are essential for maintaining chromosome stability. In humans, telomeres progressively shorten accompanying proliferation of most somatic cells, serving as "mitotic clocks" for cellular senescence. Whereas the shelterin complex provides both structural protection and length regulation for telomeres, telomerase expression, particularly the transcription of the *hTERT* gene encoding telomerase reverse transcriptase, is critical for telomere length homeostasis (1–3). The *hTERT* gene is expressed during embryonic development and in tissues containing abundant stem cells, such as the testes, ovaries, skin, and the thymus, but its expression is very low in most adult tissues (4, 5).

Transcriptional regulation of the *hTERT* gene is a complex process. Several transcription factors (TFs) have been implicated in hTERT regulation via their binding sites at its proximal promoter, including c-Myc, USFs, Sp1, and ETS family proteins (6–9). However, the dominant mode of hTERT regulation was transcriptional repression because the *hTERT* locus was embedded in a nuclease-resistant chromatin domain and its promoter was stringently repressed in a histone deacetylase–dependent manner in somatic cells (10, 11). However, high telomerase activity is found in most cancer cells (12, 13). Recent studies have shown that hTERT activation in cancer cells was associated with promoter mutations that gave rise to new binding sites for ETS family TFs (14–16). These mutations abrogated hTERT silencing in differentiated cells, resulting in increased telomerase activity and telomere elongation (17). Still, how hTERT transcription occurred during normal developmental and physiological processes remains to be elucidated.

The *hTERT* locus at chromosomal position 5p15.33 has been recognized as a "cancer hub" because the region contains a large number of single-nucleotide polymorphisms (SNPs) associated with multiple cancer types including cancers of the skin (especially melanoma), brain, cervix, prostate, breast, liver, bladder, pancreas, lungs, testes, and ovaries (18–22). Whereas some of these SNPs were localized to the proximal-promoter region, many cancer-associated SNPs were mapped to an independent downstream region from introns 2 to 4 within the *hTERT* locus, implying the presence of previously unknown regulatory sequences in this region (22, 23).

Repetitive sequences make up at least 45% of the human genome, and such sequences were once regarded as nonfunctional "junk DNA" and often ignored in genomic DNA analyses. Recent studies have begun to indicate that some of these "junk" sequences may possess significant functions in regulating gene expression, and genetic variations of these repetitive sequences may be the molecular basis for disease susceptibilities in humans. The *hTERT* locus contains abundant, repetitive DNA sequences including transposable elements such as long interspersed nuclear elements, short interspersed nuclear elements, and long terminal repeat retrotransposons as well as several variable number tandem repeats

Significance

Repetitive DNA sequences are abundant in the human genome, and their high variabilities contribute to genetic diversity and disease susceptibility. Here, we report that an intronic variable number tandem repeat element, VNTR2-1, is critical for the transcription of the human telomerase reverse transcriptase (*hTERT*) gene in a cell-context–dependent manner. Removal of this element at its native genomic site in cancer cells resulted in telomere shortening, cellular senescence, and impaired tumor growth. VNTR2-1 length, consisting of 53 to 160 copies of 42-bp repeats, varies widely in human populations. hTERT alleles with short VNTR2-1 are underrepresented in African American centenarians, suggesting that hTERT regulation by VNTR2-1 plays a role in human aging and tumorigenesis.

Author contributions: D.C., S.W., and J. Zhu designed research; T.X., D.C., Y.Z., J. Zhang, and F.Z. performed research; D.C., Y.Z., F.Z., and S.W. contributed new reagents/analytic tools; T.X., D.C., X.Z., G.C., and J. Zhu analyzed data; and D.C., Y.W., X.Y., G.P.R., S.G., P.L., S.W., and J. Zhu wrote the paper.

The authors declare no competing interest.

This article is a PNAS Direct Submission. J.L. is a guest editor invited by the Editorial Board.

[1]T.X. and D.C. contributed equally to this work.

[2]To whom correspondence may be addressed. Email: jiyue.zhu@wsu.edu.

This article contains supporting information online at https://www.pnas.org/lookup/suppl/doi:10.1073/pnas.2019043118/-/DCSupplemental.

Published June 21, 2021.

(VNTRs, also called minisatellites [MS]). Most of these repetitive sequences are not evolutionally conserved in mammals, and they are absent in the mouse genome. Given the substantial differences in telomerase regulation and telomere homeostasis between humans and mice (24, 25), it is conceivable that these repetitive sequences play a role in human-specific regulation of the telomerase gene.

In the current study, using bacterial artificial chromosomal (BAC) reporters that contained a 160-kb human-genomic DNA encompassing the *hTERT* gene and its neighbor loci, we found that genomic sequences outside of its proximal promoter were important for hTERT transcription. A variable DNA repeat, VNTR2-1, in intron 2 was identified as an enhancer-like element required for telomere maintenance during in vitro cell proliferation and tumor growth in nude mice. In addition, African Americans (AAs) with short VNTR2-1 alleles were underrepresented in centenarians. Our data indicated that VNTR2-1 was a polymorphic regulatory element of the *hTERT* gene and likely played a role in genetic susceptibilities to cancer and other age-related diseases.

Results

Activation of the hTERT Promoter by VNTR2-1. Previous studies have shown that the hTERT promoter was erroneously regulated in an ectopic genomic environment, suggesting that distal sequences were required for hTERT regulation (26). Hence, BAC reporters were used to uncover possible distal regulatory elements. In the BAC reporter H(wt) containing a 160-kb human-genomic sequence encompassing the *hTERT* gene and its neighboring loci (27), a *Renilla* (*Rluc*) and a *Firefly* luciferase (*Fluc*) cassette were inserted into the ATG codons of the *hTERT* and *CRR9* genes, respectively (Fig. 1*A*). Because the *CRR9* gene was ubiquitously expressed (28), the ratio of *Rluc* to *Fluc* activities was used to assess hTERT-promoter activity in this reporter. In a transgenic mouse model containing this BAC, the expression of *Rluc* activity recapitulated the hTERT expression in human tissues, indicating that this 160-kb human sequence in this BAC reporter contained sufficient regulatory sequences for hTERT regulation in human tissues (5). A set of BAC reporters with various deletions was constructed using BAC recombineering removing the entire *hTERT* gene downstream of its promoter or portions of this region (Fig. 1*A*). The hTERT-promoter activities were determined upon transient transfection of these BAC reporters into normal human foreskin fibroblasts (NHFs). NHFs expressed no detectable hTERT mRNA because the endogenous *hTERT* gene was repressed in its native chromatin environment (11). However, the hTERT promoter in transiently transfected H(wt) was highly active, as it was not subjected to such repression. As shown in Fig. 1*B*, deletion of the 40-kb region from exon 1 to exon 16 in H(ΔTERT) dramatically reduced hTERT-promoter activity. Smaller deletions, including deletions of introns 2 through 12, introns 2 through 6, or intron 2 only, had similar effects, indicating that intron 2 contained one or more regulatory elements required for efficient hTERT transcription.

Inspection of the 11-kb intron-2 sequence of the *hTERT* gene revealed that it contained several repetitive elements including two MSs, VNTR2-1 and VNTR2-2. VNTR2-1 was especially interesting because it contained a large number of E-box (enhancer box)

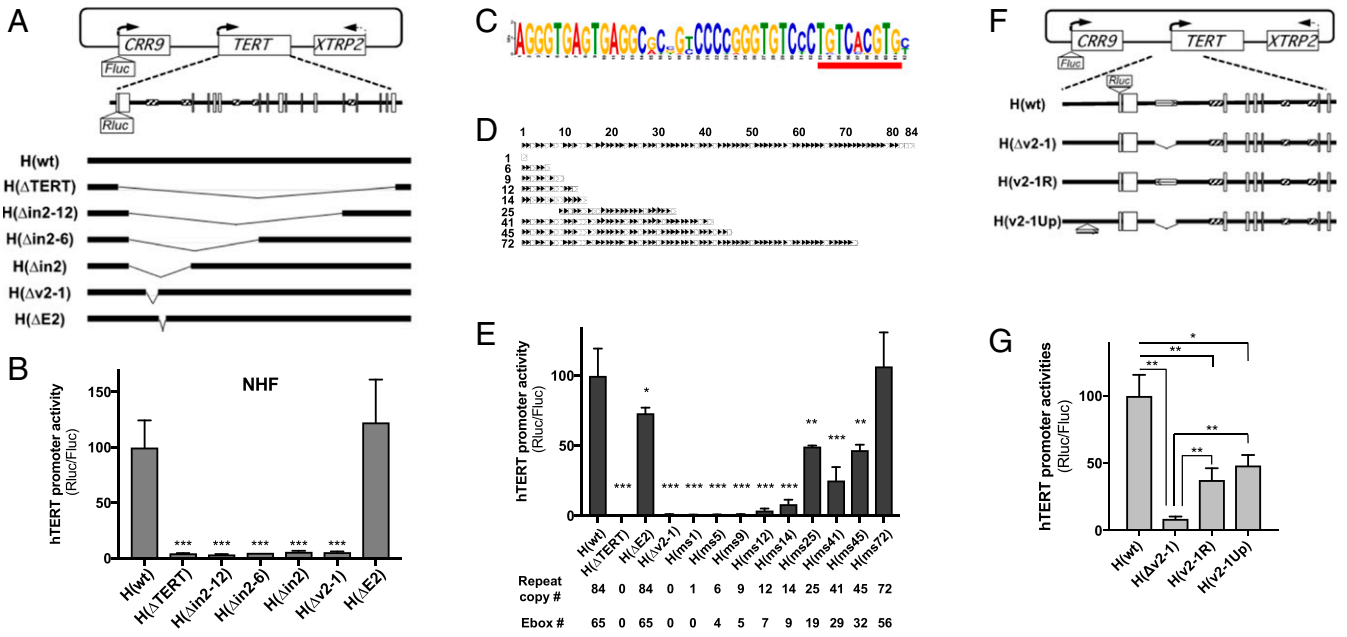

Fig. 1. Regulation of the hTERT promoter by VNTR2-1 in transient transfection assays. (*A*) BAC reporters. (*Top*) An illustration of the BAC reporter H(wt) with an expansion of the *hTERT* gene. Rectangles represent three genes, *CRR9*, *TERT*, and *XTRP2*. Vertical bars in the expansion indicate 16 exons, and horizontal hatched bars represent five VNTRs in introns 2, 6, and 13. *Fluc* and *Rluc* denote *Firefly* and *Renilla* luciferase expression cassettes, respectively. Thin lines in the lower part of the diagram represent genomic regions that are deleted in the mutant BACs. H(ΔTERT) contained a deletion of the entire *hTERT* gene from its ATG codon to the end of exon 16. H(Δin2-12) and H(Δin2-6) contained deletions of genomic sequences between exons 2 and 7 and exons 2 and 13, respectively. H(Δin2), H(Δv2-1), and H(ΔE2) contained deletions of intron 2, VNTR2-1, and a 462-bp sequence downstream of VNTR2-1, respectively. Arrows indicate promoters and directions of transcription. (*B*) Luciferase activities of BAC reporters. BACs were transiently transfected into NHFs, and luciferase activities were measured 48 h later. (*C*) Sequence variations of the 84 copies of 42-bp repeats in H(wt). The canonical E-box is underlined. (*D*) Diagrams of remaining VNTR2-1 sequences in BAC reporters with partial VNTR2-1 deletions. Each 42-bp unit is represented by a black triangle (with a canonical E-box) or a white triangle (without a E-box). (*E*) hTERT-promoter activities in BAC reporters with partial VNTR2-1 deletions. Numbers of remaining 42-bp repeats and E-boxes in the BAC reporters are shown at the bottom. The activities of mutant reporters were compared with that of H(wt) (100). (*F*) BAC reporters with VNTR2-1 at different positions and orientations. Bars with horizontal arrows represent VNTR2-1. (*G*) Effects of position and orientation of VNTR2-1 on the regulation of the hTERT promoter. BAC reporters were transfected into NHF cells, and luciferase activities were determined in 48 h. $*P < 0.05$; $**P < 0.01$; $***P < 0.001$, two-tailed Student's *t* test.

consensus sites (29). Thus, the 3.6-kb VNTR2-1 sequence was deleted in H(wt), generating H(Δv2-1). A 462-bp sequence immediately downstream of VNTR2-1 containing three E-boxes and multiple E2F consensus sites was also deleted, resulting in H(ΔE2). While the hTERT promoter in H(ΔE2) was not affected by the deletion, its activity in H(Δv2-1) decreased 10- to 30-fold. The VNTR2-1 sequence in H(wt) was determined by PacBio single-molecular real-time (SMRT) long-read sequencing and was found to consist of 84 copies of variable repeats with 42-bp unit length (Fig. 1*C*). The majority of the 42-bp repeats (65 out of 84) contained a canonical E-box (TGTCACGTG). To understand the role of these repeat sequences in hTERT activation, a series of BAC reporters with variable numbers of 42-bp repeats were generated using a modified BAC recombineering method (*SI Appendix*, Fig. S1). The deletions generally started from the 3′ end of VNTR2-1 with the exception of H(ms25) (Fig. 1*D*). Upon transient transfection in NHFs, the hTERT promoter in H(ms72), which contained 72 repeats, exhibited similar activity as H(wt) (Fig. 1*E*). However, further deletion of VNTR2-1 resulted in dramatic reduction of hTERT-promoter activity, which correlated with the length of the remaining VNTR2-1 sequence. For instance, the hTERT-promoter activity in H(ms12) containing 12 repeats and 7 E-boxes was fourfold higher than that in H(Δv2-1), whereas H(ms41) had 41 repeats and 29 E-boxes, and its hTERT promoter was 28 times more active. The only exception was H(ms25), which appeared to result from rearrangements of VNTR2-1. This reporter contained 25 repeats and 19 E-boxes, and its hTERT-promoter activity was higher than that in H(ms41). Thus, the hTERT-promoter activity in the BAC reporters generally correlated with the number of 42-bp repeats or E-boxes, suggesting that these repetitive sequences activated hTERT transcription.

To understand how VNTR2-1 functioned, the VNTR2-1 sequence was either reversed, as in H(v2-1R), or moved to 6 kb upstream of the hTERT promoter as in H(v2-1Up) (Fig. 1*F*). Upon transient transfection into NHFs, the repositioned VNTR2-1 was able to activate the hTERT promoter in both cases (Fig. 1*G*), indicating that VNTR2-1 functioned like an enhancer in a position- and orientation-independent manner. However, hTERT-promoter activities in H(v2-1R) and H(v2-1Up) were somewhat lower than those in H(wt), suggesting that the position and orientation of VNTR2-1 were necessary for the optimal TERT expression.

Association of VNTR2-1 with E-Box–Binding Proteins In Vivo. Chromatin environment of the *hTERT* locus is critical for its regulation (10, 26, 30). To study VNTR2-1 in a chromatinized setting, single-copy BAC reporters were integrated into chromosomal acceptor sites in telomerase-positive (Tel^+) and -negative (Tel^-) fibroblast lines using recombinase-mediated BAC targeting (RMBT) (27) (Fig. 2*A*). The acceptor sites were surrounded by a pair of chicken β-globin insulators, cHS4, reducing potential chromosomal positional effects (27, 31). In this setting, deletion of intron 2 or VNTR2-1 reduced hTERT-promoter activity fivefold in Tel^+ cells. Although VNTR2-1 deletion also reduced TERT transcription in Tel^- cells, the difference was not statistically significant because the luciferase counts in Tel^- cells were very low.

VNTR2-1 contained a large number of canonical E-boxes, potential binding sites for the basic helix–loop–helix leucine zipper (bHLH-LZ) family TFs such as c-Myc/Max and upstream stimulatory proteins 1 and 2 (USF1/2) (32). Hence, chromatin immunoprecipitation (ChIP) qPCR assays were performed to determine whether VNTR2-1 was associated with these proteins. Because VNTR2-1 contained tandem repeats, PCR amplicons could only be designed at two ends (c and d in Fig. 2*B*). As shown in Fig. 2*C*, both USF1 and USF2 antibodies pulled down amplicons c and d in Tel^+ cells; their binding to VNTR2-1 was stronger than to the hTERT promoter, which contained at least two E-boxes. Knocking down either USF1 or USF2 by small hairpin RNAs (shRNAs) reduced the binding signals of both USF1 and USF2, indicating that USF1 and USF2 bound to VNTR2-1 as heterodimers (Fig. 2 *C* and *D*). As compared with USF1/2, more Max bound to the hTERT promoter than to VNTR2-1. Knockdown of the Max protein by an shRNA nearly eliminated its binding to these regions. No significant binding of the c-Myc protein to either the hTERT promoter or VNTR2-1 was detected. Moreover, knockdown of USF1 increased Max binding to the hTERT promoter and VNTR2-1, suggesting that USF1 competed with Max for binding to these regions. The association of these TFs to the *hTERT* locus was weaker in Tel^- cells than in Tel^+ cells (*SI Appendix*, Fig. S2), consistent with previous data indicating that the hTERT promoter was less accessible to TFs in Tel^- cells (33).

The binding of TFs to VNTR2-1 was also assessed by using datasets available from the Encyclopedia of DNA Elements (ENCODE). ChIP-sequencing (ChIP-seq) datasets of several E-box binding proteins in K562 human myelogenous leukemia cells were aligned to the *hTERT* locus. K562 cells contain about 120 copies of 42-bp repeats in both alleles and express a high level of hTERT mRNA (34). As shown in Fig. 2*E*, USF1 and, to a lesser extent, USF2 were enriched at VNTR2-1 but not at the hTERT promoter. Max, but not c-Myc, was enriched at both the hTERT promoter and VNTR2-1. As a control, c-Myc bound to two regions of the upstream *CLPTM1L* (*CRR9*) gene in the same datasets. These data were consistent with our ChIP-PCR data in Tel^+ fibroblasts and indicated that VNTR2-1 was associated with bHLH-LZ family TFs in vivo.

Involvement of Both Promoter E-Boxes and VNTR2-1 in hTERT Activation. Previous studies showed that two canonical E-boxes at -165 nt and +44 nt relative to the transcription start site (TSS) of the hTERT promoter mediated its regulation via bHLH proteins (8, 35). Thus, we studied how these two promoter E-boxes and VNTR2-1 functioned together to activate hTERT transcription. In our previous report (9), these two E-boxes in H(wt) were mutated, resulting in EboxDM. Here, VNTR2-1 in the BAC EboxDM was deleted using BAC recombineering to generate DM/Δv2-1. In transiently transfected NHF cells, whereas VNTR2-1 deletion (Δv2-1) resulted in a dramatic loss of hTERT-promoter activity, EboxDM had no effect on hTERT-promoter activity (Fig. 3*A*). However, in chromatinized BAC reporters in Tel^+ cells, either EboxDM or Δv2-1 led to a significant decrease of hTERT-promoter activity. EboxDM and Δv2-1 together (DM/Δv2-1) resulted in a nearly complete loss of hTERT-promoter function, indicating that both VNTR2-1 and promoter E-boxes were required for hTERT transcription in the chromatinized setting (Fig. 3*B*). Overexpression of USF2, not USF1, increased hTERT-promoter activity in chromatinized H(wt), EboxDM, and H(Δv2-1), suggesting that USF2 activated hTERT promoter via either promoter E-boxes or VNTR2-1 (Fig. 3*C*). c-Myc alone increased the activity of wild-type hTERT promoter in H(wt) and H(Δv2-1) but not the hTERT promoter containing EboxDM mutations, indicating that c-Myc acted through two promoter E-boxes (Fig. 3*D*). Overexpression of both c-Myc and Max stimulated the EboxDM mutant promoter in the presence of VNTR2-1, suggesting that c-Myc/Max could also activate the hTERT promoter via VNTR2-1. Finally, none of the E-box–binding TFs activated the hTERT promoter in the BAC reporter DM/Δv2-1. Taken together, the data indicated that hTERT regulation by bHLH TFs was mediated by both the distal VNTR2-1 and E-boxes at the proximal promoter.

Function of VNTR2-1 during Embryonic Stem Cell Differentiation. The *hTERT* gene was highly expressed in pluripotent stem cells but down-regulated upon differentiation (36, 37). To study hTERT regulation in such cells, single-copy BAC reporter H(wt) was integrated into mouse embryonic stem cell (ESC) acceptor line T2-5 by RMBT (26). As we reported previously (26, 38), the hTERT

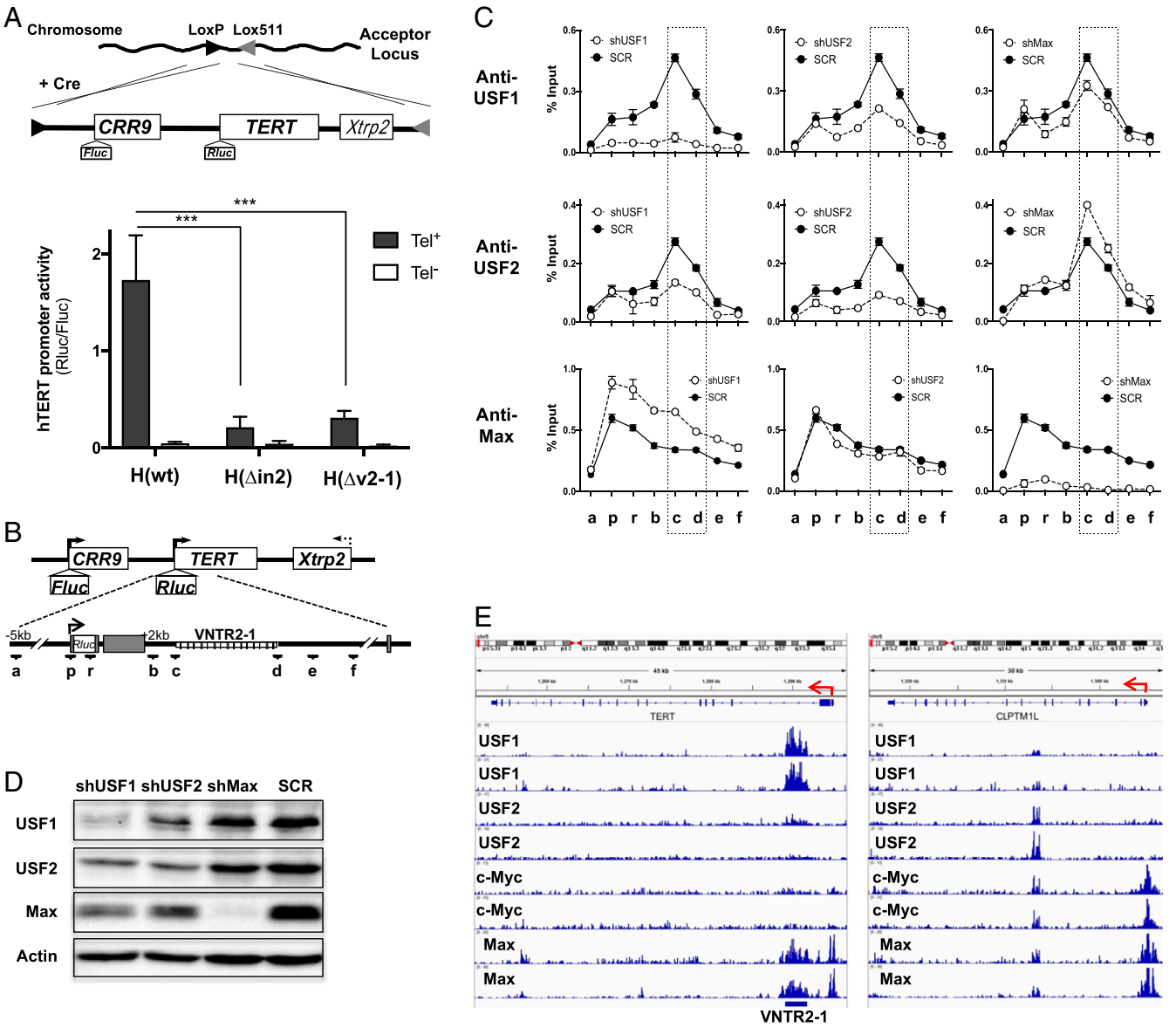

Fig. 2. Regulation of the hTERT promoter by VNTR2-1 in chromatinized BAC reporters. (*A*) hTERT-promoter activity in chromatinized BAC reporters. (*Top*) A diagram of Cre-mediated integration of BAC reporters into a chromosomal acceptor locus. LoxP and Lox511 sites are represented by black and gray triangles, respectively. (*Bottom*) Activities of chromatinized hTERT promoters in Tel$^+$ and Tel$^-$ cells. The BAC integration in all clones was validated via Southern blotting and sequencing of the junctions (27). (*B*) A diagram of the genomic region from the hTERT promoter to intron 2 in H(wt). Gray boxes are exons 1, 2, and 3. Exon 1 is interrupted by an *Rluc* cassette. VNTR2-1 is shown as a hatched bar. Positions of PCR amplicons used in ChIP experiments are indicated by a through f. (*C*) TF binding to the *hTERT* locus in chromatinized H(wt) in Tel$^+$ cells. Tel$^+$ cells containing chromatinized H(wt) were transduced with lentiviral shRNAs against TFs or scrambled RNA controls for 4 d. Chromatin fragments were precipitated using antibodies against TFs, followed by qRT-PCR analyses. VNTR2-1 regions are highlighted by dashed boxes. (*D*) Western analyses showing knockdown of E-box–binding TFs in Tel$^+$ cells. (*E*) Association of VNTR2-1 with E-box–binding TFs in K562 cells. Chromatin occupancy data at the *hTERT* locus (hg38 chr5:1,253,287-1,295,162) and the upstream *CLPTM1L* gene [hg38 chr5:1,318,000-1,345,002] are shown on the left and right, respectively. ChIP-seq data are from ENCODE datasets ENCFF523RSS, ENCFF070DTB, ENCFF424FKD, ENCFF241NUY, ENCFF191PXA, ENCFF936GCU, ENCFF393FKW, and ENCFF535RJW, correspond to USF1 (replicates 1 and 2), USF2 (1 and 2), c-Myc (1 and 2), and Max (1 and 2) (from top to bottom) (63). The horizontal bar at the bottom indicates the genomic position of VNTR2-1. Promoters and transcriptional directions are indicated by red arrows.

promoter in H(wt) was highly active in ESCs and progressively down-regulated over 100-fold during differentiation via embryoid bodies (EBs) into fibroblast-like cells (Fig. 4*A*). To determine the function of VNTR2-1 in ESCs, H(Δv2-1) was integrated into the same acceptor site in T2-5 cells by RMBT. Surprisingly, the hTERT promoters in H(wt) and H(Δv2-1) were similarly active in ESCs, indicating that hTERT transcription in ESCs did not require VNTR2-1. However, hTERT-promoter activity was lower in H(Δv2-1) than in H(wt) during EB differentiation (Fig. 4*A*). During EB differentiation, pluripotency markers Oct4 and Nanog rapidly decreased, and differentiation marker AFP was similarly elevated in differentiating EBs for all clones (*SI Appendix*, Fig. S3), indicating that lower hTERT-promoter activities in H(Δv2-1) was not due to inefficient differentiation. In fully differentiated fibroblast-like cells, the hTERT promoter was silenced in both H(wt) and H(Δv2-1). Therefore, while VNTR2-1 did not affect the hTERT-promoter activity in either ESCs or fully differentiated cells, it functioned to maintain hTERT transcription during ESC differentiation.

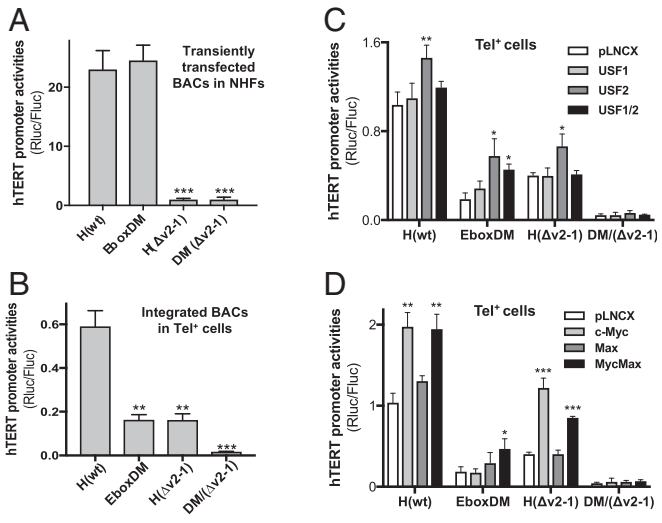

Fig. 3. Involvement of promoter E-boxes and VNTR2-1 in the regulation of the hTERT promoter. (*A*) hTERT activation by promoter E-boxes and VNTR2-1 in transient transfection assays. NHFs were transiently transfected with BAC reporters, and luciferase activities were measured in 48 h. EboxDM, H(wt) with mutations at two promoter E-boxes; DM/(Δ2-1), the BAC reporter containing the promoter E-box mutations and VNTR2-1 deletion. (*B*) hTERT regulation in chromatinized BAC reporters. All BAC reporters were integrated at the same chromosomal site in Tel$^+$ cells. Luciferase activities were measured in proliferating cells. (*C* and *D*) Regulation of the hTERT promoter in chromatinized BAC reporters by USF1/USF2 (*C*) and c-Myc/Max (*D*). Tel$^+$ cells with stably integrated BAC reporters were transiently transfected with plasmids expressing TFs, and luciferase activities were determined in 48 h. All luciferase activities in cells overexpressing TFs were compared with the respective pLNCX vector controls: $*P < 0.05$; $**P < 0.01$; $***P < 0.001$, two-tailed Student's *t* test.

The chromatin states of VNTR2-1 in ESCs and differentiated cells were examined by ChIP-qPCR analyses. As shown in Fig. 4*B*, c-Myc primarily bound to the hTERT promoter, and USF1 and USF2 were enriched at VNTR2-1 in ESCs. On the other hand, Max was associated with both the promoter and VNTR2-1. The association of these TFs was greatly reduced upon differentiation of ESCs into fibroblast-like cells, indicating that the binding of these TFs to both the proximal promoter and VNTR2-1 correlated with hTERT transcription. Covalent histone modifications at the 5′ half of the *hTERT* locus were also examined. Whereas H3K4me2 and H3K4me3 were enriched around the hTERT promoter, the VNTR2-1 region contained a high level of H3K4me1, an epigenetic marker of enhancer (Fig. 4*C*). This enrichment of H3K4me1 at VNTR2-1 was lost in differentiated cells. Additionally, the hTERT promoter was associated with acetylated H3K27 in ESCs but not in differentiated cells. In differentiated cells, the entire 5′ half of the *hTERT* locus, including the hTERT promoter and VNTR2-1, was covered by H3K27 trimethylation, consistent with silencing of the *hTERT* gene in these cells. Taken together, these data indicated that VNTR2-1 functioned as an enhancer-like element to maintain hTERT transcription during ESC differentiation.

Telomere Homeostasis in Cell Lines with Genomic Deletion of VNTR2-1. To study how VNTR2-1 functioned at its native genomic location, Southern analysis was performed to measure its length in commonly used human cell lines by cleaving genomic DNAs at two PvuII sites just outside of VNTR2-1. The VNTR2-1 length was polymorphic, ranging from 3 to 6 kb in these cells (*SI Appendix*, Fig. S4). Most cells had VNTR2-1 of two different lengths, but some had only one band corresponding to VNTR2-1 sizes of two *hTERT* alleles.

In order to perform the genomic deletion experiment, karyotypes of telomerase-expressing cell lines were analyzed. While most cancer cells were polyploidy with more than two *hTERT* genes, the melanoma cell line MelJuSo and HEK293 cells were near diploid and contained two *hTERT* alleles. Hence, we chose to use these cell lines to perform CRISPR-mediated genomic deletions. From a total of 76 independent clones isolated from MelJuSo cells transfected with single-guide RNAs (sgRNAs) targeting two sides of VNTR2-1, two clones, J1 and J52, with deletions in both *hTERT* alleles were identified for further analysis. VNTR2-1 was deleted at both alleles in J1 cells, resulting in complete loss of the 5.6-kb SphI band detected by the MS probe (Fig. 5 *A* and *B*). The hTERT mRNA level in J1 cells was 10-fold lower than in unedited MelJuSo cells, accompanied by a marked decrease of telomerase activity (Fig. 5 *C* and *D*). In clone J52, VNTR2-1 was deleted entirely at one allele and partly at the other allele, leaving behind a 1.9-kb SphI band detectable by both MS and HS4 probes (Fig. 5 *A* and *B*). PCR amplification and sequencing of the deletion junction revealed that there remained five copies of 42-bp repeats (containing three E-boxes) in the partially deleted allele. The hTERT mRNA level and telomerase activity also decreased in J52 cells, albeit not as dramatically as those in J1 cells (Fig. 5 *C* and *D*). Transduction of these clones with a retrovirus containing an hTERT complementary DNA (cDNA) restored the hTERT mRNA level and telomerase activity. Sequencing of the hTERT promoters in MelJuSo cells revealed that one of the *hTERT* alleles contained both C250T and C228T cancer-specific mutations. These results indicated that VNTR2-1 activated hTERT expression at its native genomic location, and this activation occurred regardless of whether the promoter contained cancer-specific mutations.

The activation of hTERT transcription by VNTR2-1 is likely associated with chromatin changes at the promoter. Thus, ChIP experiments were performed to determine the impact of VNTR2-1 deletion on the hTERT promoter. As shown in *SI Appendix*, Fig. S5, the binding of USF1 and Max to the hTERT promoter was decreased in J1 cells compared with that in a clone of MelJuSo cells with intact VNTR2-1. Genomic deletion of VNTR2-1 in J1 cells was also associated with reduced H3K4me2 and H3K4me3 at the hTERT promoter, consistent with the decreased hTERT transcription in J1 cells.

Next, we set out to determine how VNTR2-1 deletions impacted telomere homeostasis and cell proliferation by passaging J1, J52, and a MelJuSo clone with two intact VNTR2-1 for over 100 population doublings (PDs) (Fig. 5*E*). Whereas unedited MelJuSo cells propagated continuously, proliferation of J1 cells slowed down after about 50 PDs and came to a complete halt after 63 PDs, coinciding with significantly shortened telomeres (Fig. 5*F*). Upon transduction of the hTERT retrovirus, J1 cells displayed elongated telomeres and continued to proliferate beyond 110 PDs (Fig. 5 *E* and *F*). J52 cells initially proliferated more slowly than both unedited MelJuSo and J1 cells; their proliferation slowed down only slightly after 100 d in culture compared with J52 cells transduced with the hTERT retrovirus (Fig. 5*E*). J52 cells had short telomeres even at PD 16, and their telomeres became elongated upon hTERT overexpression (Fig. 5*F*). In addition, we also performed a colony-formation assay, in which vector or hTERT retrovirus–transduced cells were plated into Petri dishes and cultured for 3 wk. J1 and J52 cells also formed smaller colonies compared with unedited MelJuSo cells (Fig. 5*G*). Transduction by the hTERT retrovirus restored their colony-forming abilities. These data indicated that genomic deletion of VNTR2-1 resulted in short telomeres and limited the proliferative capability of MelJuSo cells.

Because short telomere–induced proliferation arrest was often associated with cellular senescence, MelJuSo cells with or without VNTR2-1 deletions were examined for the expression of senescence markers. Both J1 and J52 cells, but not unedited MelJuSo cells, expressed senescence-associated (SA) β-galactosidase activity,

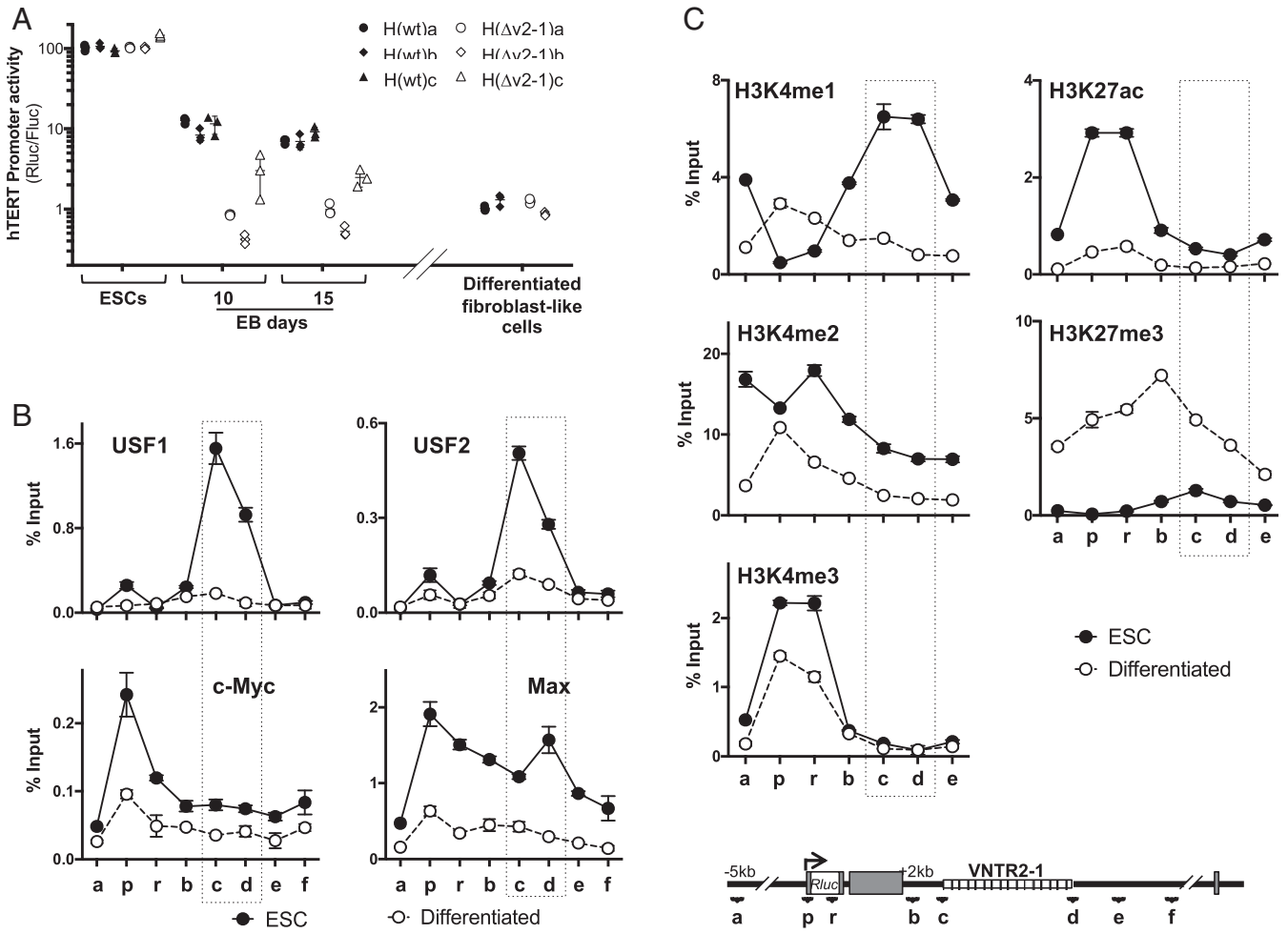

Fig. 4. Regulation of the hTERT promoter by VNTR2-1 during differentiation of mouse ESCs. (*A*) hTERT-promoter activities of chromatinized BAC reporters in ESCs. Single-copy H(wt) and H(Δv2-1) were integrated at the same acceptor sites in ESCs. Luciferase activities were determined in proliferating ESCs, in individual EBs at days 10 and 15 after initiation of differentiation, and in differentiated fibroblast-like cells. Three independently derived ESC clones containing each BAC were used for EB differentiation. Two clones for each BAC, a and b, were further differentiated into fibroblast-like cells. hTERT-promoter activities are shown as ratios of *Renilla* to *Firefly* luciferase activities. (*B* and *C*) TF binding (*B*) and histone modifications (*C*) within the *hTERT* locus. Chromatin fragments from ESCs and in vitro–differentiated fibroblast-like cells were immunoprecipitated with antibodies against TFs or specific histone modifications, followed by qRT-PCR analyses. A diagram of genomic positions a through f is shown below *C*. VNTR2-1 regions are highlighted by dashed boxes.

which decreased upon hTERT overexpression (Fig. 5*H*). MelJuSo cells also expressed senescence-associated proteins p53 and p21 but not $p16^{Ink4a}$; p21 levels in J1 and J52 cells were higher than those in unedited MelJuSo cells, and they decreased upon hTERT overexpression (Fig. 5*I*). Taken together, these data indicated that VNTR2-1 regulated telomere homeostasis, cellular proliferation, and senescence in MelJuSo cells.

To determine the role of VNTR2-1 in HEK293 cells, VNTR2-1 in these cells was also deleted using the same strategy. Two independent clones, ΔMS#1 and ΔMS#2, with VNTR2-1 deletion at both *hTERT* alleles and another clone without VNTR2-1 deletion were analyzed (*SI Appendix*, Fig. S6 *A* and *B*). Homozygous VNTR2-1 deletion resulted in 50 and 70% reductions of hTERT mRNA levels in ΔMS#1 and ΔMS#2, respectively, and telomere shortening (*SI Appendix*, Fig. S6 *C* and *D*). hTERT overexpression increased telomerase activities and telomere lengths in all clones. However, these changes did not affect proliferation of HEK293 cells for over 250 PDs (*SI Appendix*, Fig. S6*E*). These data indicated that, while VNTR2-1 activated endogenous hTERT transcription in HEK293 cells, the reduced telomerase activities following VNTR2-1 deletion were still sufficient to maintain the continuous proliferation of these cells.

VNTR2-1 and Tumor Growth In Vivo. Next, we evaluated the role of VNTR2-1 in tumor development in a xenograft melanoma model using MelJuSo cells. J52 and the unedited MelJuSo clone at passage 5 following transduction of the hTERT or vector retroviruses were injected subcutaneously into nude mice; J1 cells at passage 3 after retroviral transduction were used because their proliferation slowed down more quickly (Fig. 5*E*). As shown in Fig. 5*J*, tumors started to appear between 9 and 13 d after cell implant. Injections of unedited MelJuSo and J1/hTERT cells led to tumor formation within 24 d, and tumors grew rapidly until day 63, when the mice were killed due to advanced tumor burden (Fig. 5*K* and *SI Appendix*, Fig. S7*A*). Yet 5 out of 13 injections of J1/pBABE cells failed to result in measurable tumors for at least 40 d. All J1/pBABE-induced tumors grew slowly; no tumors reached 200 mm^3 in 63 d, and several tumors dissipated after initial detection and growth. The growth rates of J52 tumors were also slower than unedited MelJuSo cells. Following transduction of the hTERT retrovirus, J52 tumors grew significantly faster, albeit not as fast as unedited MelJuSo cells or J1/hTERT cells. In addition, whereas tumors derived from all cells were histologically similar, J1 and J52 tumors exhibited a decreased expression of proliferation marker Ki-67 as compared with unedited MelJuSo tumors, and hTERT overexpression restored Ki-67

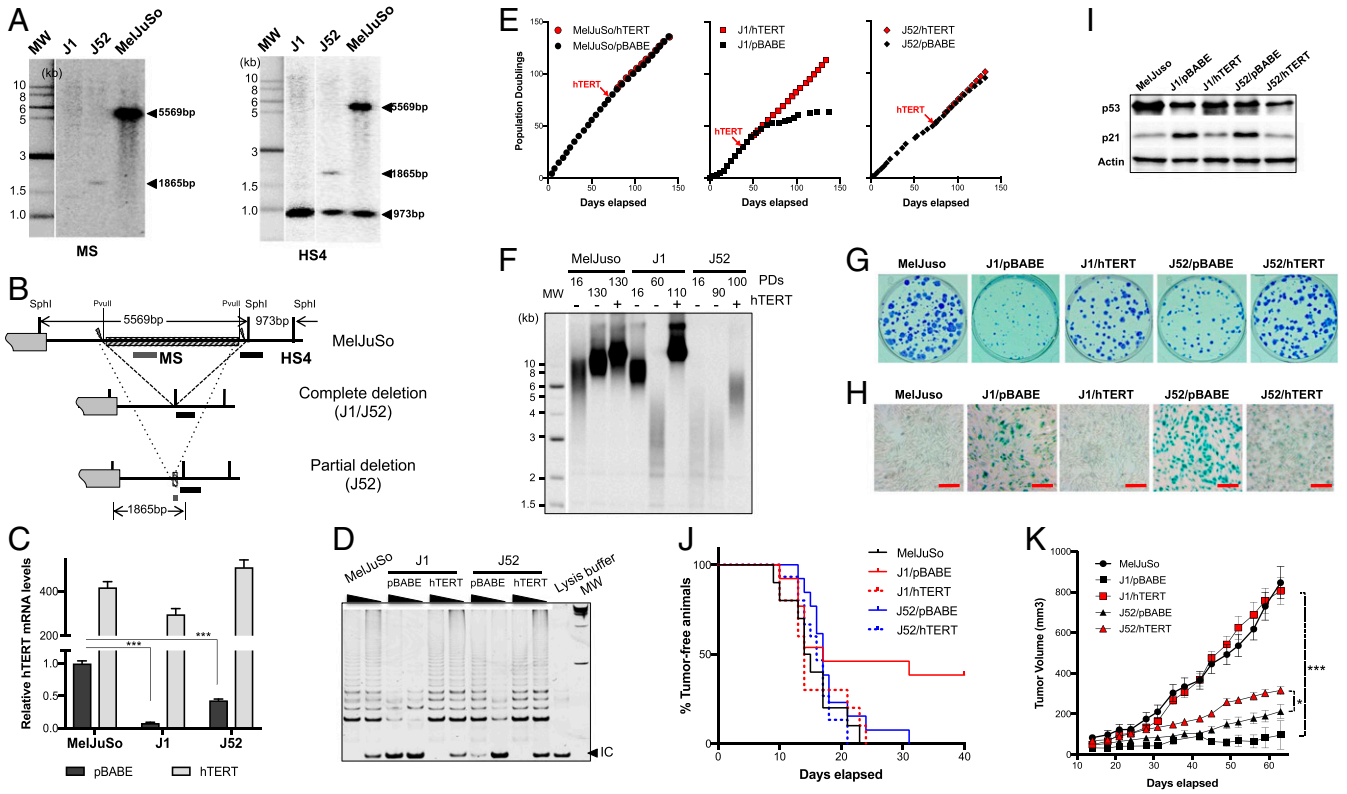

Fig. 5. Effects of genomic VNTR2-1 deletion on telomere homeostasis, cellular proliferation, and tumor growth. (*A* and *B*) Characterization of CRISPR-mediated VNTR2-1 deletion. MelJuSo cells were transfected with two pX458-sgRNAs targeting two sides of VNTR2-1. (*A*) Genomic DNAs from MelJuSo cell lines were digested with SphI, followed by Southern analysis. MW, molecular weight markers in kilobases. Sizes of fragments detected are indicated on the right. (*B*) Diagrams interpreting the results of Southern blots in *A*. The gray rectangles show exon 2 of the *hTERT* gene, and the hatched rectangles represent VNTR2-1. Probes and their positions are indicated as gray horizontal bars (MS) and black bars (HS4). Flash signs, sgRNA cleavage sites. Clone J1 contained two alleles with complete VNTR2-1 deletion, whereas J52 had one allele with complete VNTR2-1 deletion and another allele with a partial deletion. The partially deleted VNTR2-1 was recognized as a weak 1865-bp band by both MS and HS4 probes. (*C*) hTERT mRNA levels. MelJuSo clones with or without VNTR2-1 deletions were infected with retroviruses pBABE or pBABE-hTERT, followed by selection for puromycin resistance for 7 d and isolation of total RNAs. hTERT mRNA levels were determined by qRT-PCR analysis and normalized to 18S rRNA. (*D*) Telomerase activities. Extracts of 1,000 and 200 cells were used to measure telomerase activity by TRAP assay. IC, internal control. (*E*) Proliferation of MelJuSo cells. Cells (5×10^4 per well) were seeded into 6-well plates and passaged when they reached 80 to 90% confluence. Each cell line was transduced with pBABE or pBABE-hTERT retroviruses at times indicated by red arrows. Pools of transduced cells were passaged independently. (*F*) Telomere restriction fragments in MelJuSo cells. Cells were transduced with retroviruses as shown in *E* and harvested at indicated PDs. Genomic DNAs were digested with Hinf I and Rsa I, followed by Southern blotting, and probed with biotinylated $(TTAGGG)_3$. (*G*) Colony formation. At five passages after retroviral transduction, 200 cells were seeded into each well of 6-well plates and cultured for 21 d. Colonies were stained via 0.5% crystal violet. (*H*) Expression of SA (senescence-associated) acidic β-galactosidase activities. MelJuSo cells were plated in 6-well plates after 10 passages following retroviral transduction and stained for acidic β-galactosidase. (Scale bars, 200 μm.) (*I*) Expression of SA proteins. Protein extracts were harvested from MelJuSo cells at the 10th passages following retroviral transduction. Proteins were detected in Western blots using antibodies indicated on the left. (*J*) Kaplan–Meier tumor-free curves. At passage 5 after transduction of pBABE or pBABE-hTERT retroviruses (passage 3 for J1 cells), 2×10^6 cells were injected subcutaneously into nude mice, and tumor formation was monitored. MelJuSo clone with intact VNTR2-1, $n = 10$; J1, $n = 13$; J1/hTERT, $n = 10$; J52, $n = 13$; J52/hTERT, $n = 15$. Tumors were never detected at five of the J1 injection sites. (*K*) Tumor-growth curves (mean ± SEM). Averages of tumor sizes at days after injection are shown. $^*P < 0.05$; $^{**}P < 0.01$; $^{***}P < 0.001$, two-tailed Student's *t* test.

expression (*SI Appendix*, Fig. S7 *B* and *C*). Thus, reduced hTERT expression as a result of VNTR2-1 deletion impaired tumor growth in vivo, suggesting that VNTR2-1 was required for efficient tumor development.

Variation of VNTR2-1 Length in Human Populations. To assess the genetic polymorphism of VNTR2-1 in human populations, we analyzed genomic DNA samples of 99 Caucasian Americans (CAs) and 77 AAs from control groups enrolled in the Georgia Centenarian Study ranging in age from 20 to 59 y old (39). VNTR2-1 lengths in all samples were determined by Southern blotting, and Fig. 6*A* showed 10 random samples from each group. The result revealed that CAs had a VNTR2-1 length of 3 to 7 kb, but VNTR2-1 lengths in AAs were more diverse, and many samples had VNTR2-1 fragments of less than 3 kb. The data indicated that there were significant variations of VNTR2-1 length within human populations.

The VNTR2-1 sequences were also investigated by sequencing analysis. Because most sequencing methods produced short reads and were not suitable for sequencing repetitive DNAs, the PacBio SMRT method, capable of sequencing long repetitive DNAs (40), was used to sequence VNTR2-1 in genomic DNA samples. The data revealed that the sizes of VNTR2-1 in 176 samples ranged from 53 to 160 copies of a 42-bp repeat. Whereas individual repeat units had variable sequences, with a consensus sequence shown in Fig. 6*B*, the unit length was exactly 42 bp in all samples. Among 99 CA samples, the most frequent alleles had 84 (37.5%), 117 (15.0%), and 86 repeats (13.0%). In 77 AA samples, the most common alleles were 84 and 64 repeats (13.0% each) followed by 76 and 87 repeats (9.1% each). There were also rare alleles that occurred as rarely as only once. The vast majority of VNTR2-1 sequences within each size group were identical, suggesting that recombination between two VNTR2-1 alleles had been infrequent in modern-day humans. Interestingly, all VNTR2-1 alleles in CAs contained 76 or more

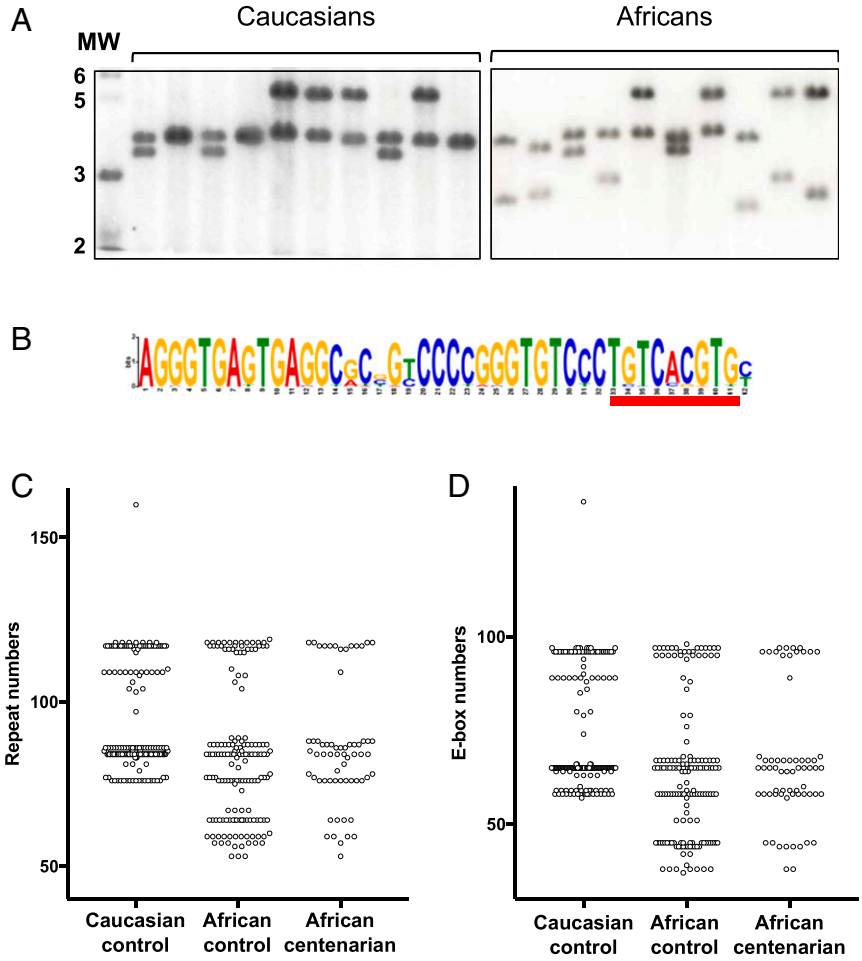

E

VNTR2-1 length	AA controls (n=77)	AA centenarians (n=32)	OR (95% CI)	*P*- value
Genotype association				
LL	33 (43%)	22 (69%)		
LS + SS	44 (57%)	10 (31%)	**0.34 (0.14-0.82)**	**0.014**
LS	*39*	*10*		
SS	*5*	*0*		
Allelic association				
L	105 (68%)	54 (84%)		
S	49 (32%)	10 (16%)	**0.40 (0.16-0.93)**	**0.014**

Fig. 6. Genetic diversities of VNTR2-1 in CAs and AAs. (*A*) Length variations of VNTR2-1 in CAs and AAs. Genomic DNAs were digested with PvuII and analyzed on Southern blots using VNTR2-1–specific probe MS. A total of 10 samples from each group are shown. (*B*) Consensus sequence of 42-bp repeats. The sequence logo represents the consensus sequence of 42-bp repeats among 99 CAs and 77 AAs. The canonical E-box is underlined by a red bar. (*C* and *D*) Lengths of VNTR2-1 among CA and AA controls, as well as AA centenarians, in numbers of 42-bp repeats (*C*) and E-boxes (*D*). (*E*) Association of VNTR2-1 length with longevity among AAs. LL, LS, and SS are genomic DNA samples with two long, a long and a short, and two short VNTR2-1 alleles, respectively. L, alleles with 76 or more copies of 42-bp repeats; S, alleles with less than 76 copies. OR, odds ratio. *P* values are calculated via two-tailed χ^2 test.

repeats, whereas 32% of VNTR2-1 alleles in AAs had fewer than 76 repeats (Fig. 6*C*). Similarly, when E-box numbers were counted, all CA alleles had 57 or more E-boxes, and one-third of AA alleles had fewer than 57 E-boxes (Fig. 6*D*). These data indicated that the shorter VNTR2-1 alleles, and thus fewer numbers of 42-bp repeats, were likely unique to African origins.

VNTR2-1 Length in AA Centenarians. Telomere-length homeostasis has been linked to human longevity (41). To study the potential roles of VNTR2-1 in human aging, genomic DNA samples from AA centenarians enrolled in the Georgia Centenarian Study (n = 32, ages 98 to 108) (39) were sequenced and compared with the matching AA controls (n = 77, ages 20 to 59) (Fig. 6*C*). Based on earlier data, we defined long VNTR2-1 alleles (L) as those containing 76 copies or more of 42-bp repeats, which were present in both AAs and CAs, and we defined short alleles (S) as those with 53 to 73 repeats, which were found predominantly among AAs. As shown in Fig. 6*E*, there were fewer AA centenarians with at least

one short VNTR2-1 allele (LS + SS) compared with the control group (odds ratio [OR] = 0.34; $P = 0.014$). When calculated by allelic association, there were also fewer S alleles among AA centenarians (OR = 0.40; $P = 0.014$). Therefore, individuals with at least one S VNTR2-1 allele were less likely to be a centenarian, suggesting an important role of VNTR2-1 in human aging.

Discussion

Multiple tandem DNA repeats within the *hTERT* gene were previously reported (29, 42). In this study, we identified intronic VNTR2-1 as an enhancer-like distal regulatory element of the *hTERT* gene and presented evidence for its involvement in regulating telomere homeostasis during cellular proliferation, differentiation, and tumorigenesis. First, VNTR2-1 bound to bHLH TFs and activated hTERT transcription in normal human fibroblasts, transformed fibroblasts, and differentiated ESCs in experiments using either transiently transfected or chromosomally integrated BAC reporters. Second, the activation by VNTR2-1 appeared to be dependent on repeat copy numbers, although the order of repeats might also affect its activity. VNTR2-1 was able to activate hTERT transcription when it was placed upstream of the hTERT promoter or in a reverse orientation. Third, genomic deletion of VNTR2-1 resulted in decreased hTERT mRNA expression and telomerase activity and progressive telomere shortening in host cells. Lastly, in ESCs, VNTR2-1 was enriched with H3K4me1 but not H3K4me3, an epigenetic hallmark of enhancers (43, 44).

While enhancers are common regulatory elements, VNTR2-1 is unique because it consists of a large and variable number of 42-bp repeats. Such repeat sequences are prone to change, and their mutation rates are several orders of magnitude higher than most genomic sequences. Thus, they are important sources of genomic instability and are associated with developmental disorders and disease susceptibilities (45). Recent studies have shown that repetitive DNA sequences could play vital roles in gene regulation. For example, rearrangement of an MS-like sequence upstream of the *MYB10* gene promoter resulted in the autoregulation of the MYB10 TF and increased levels of anthocyanin that produce red foliage and red fruit flesh in apple trees (46). It was also reported that recruitment of the ZEB1 transcriptional repressor to its binding motifs in tandem repeats promoted the maintenance of mesenchymal identity in cancer cells (47). In the current study, we show that genomic deletions of VNTR2-1 led to a reduction of telomere length, induction of cellular senescence in MelJuSo cells, and impairment of xenograft melanoma growth. VNTR2-1 deletions did not affect hTERT transcription in undifferentiated ESCs, consistent with the data that showed that the hTERT promoter was in an open chromatin environment in pluripotent stem cells (24, 37). The enrichment of bHLH TFs and H3K4me1 at VNTR2-1 in ESCs suggests that it may exist as a poised element in undifferentiated cells. Upon differentiation, the chromatin region of the *hTERT* gene became compacted and repressed (36); maintaining hTERT transcription in differentiating cells might therefore require cooperation between VNTR2-1 and its promoter. Indeed, the hTERT promoter in the wild-type BAC reporter H(wt) remained active in differentiating EBs until cells became fully differentiated, whereas the hTERT promoter in the mutant BAC reporter lacking VNTR2-1 was rapidly inactivated upon EB differentiation. This suggested that VNTR2-1 might be involved in maintaining telomerase expression in somatic stem cells.

The consensus sequence of the 42-bp repeats in VNTR2-1 contains several potential TF binding sites, of which the most prominent is a canonical E-box, the binding site for many bHLH-family TFs. It was previously reported that c-Myc/Max activated hTERT transcription via E-boxes at the proximal promoter (6, 35). Our data indicated that E-boxes at both the promoter and VNTR2-1 were crucial for hTERT regulation by c-Myc/Max and USF1/2 (Fig. 3). Interestingly, USF1/2 preferentially bound to VNTR2-1, and c-Myc bound primarily to the hTERT promoter, but Max associated with both the proximal promoter and VNTR2-1, suggesting different roles of the promoter and VNTR2-1 in hTERT regulation mediated by these bHLH TFs. Max may bind to VNTR2-1 as a repressive homodimer or a repressive heterodimer with Mxd1 or other Myc super family members (48). Yet VNTR2-1 deletion did not increase hTERT-promoter activity in any of the cells tested including telomerase-negative cells. Hence, the role of Max binding to VNTR2-1 remained to be elucidated. It is possible, however, that VNTR2-1 might function as a repressive element by binding to repressor proteins in certain somatic cells. It was shown, in the case of ZEB1, that highly clustered E-boxes could promote cooperative recruitment of bHLH TFs, resulting in an all-or-none mode of activation (47). Alternatively, multiple TFs might bind individual E-boxes independently. The overall TF occupancy of E-boxes determined by nuclear concentrations of bHLH TFs controlled the hTERT-activation status in an analog fashion. The latter mechanism provided an opportunity to fine-tune hTERT transcription.

VNTR2-1 is an evolutionarily new acquisition present in apes and old-world monkeys but absent in new-world monkeys and prosimians (*SI Appendix*, Fig. S8). In humans, while the repeat number varies, the 42-bp unit length is strictly conserved with minor variations in repeat sequences. VNTR2-1 in chimpanzees is similar to that in humans both in unit length and repeat sequences. However, sequences and repeat lengths of VNTR2-1 are more variable in other primates including bonobos, gorillas, gibbons, and old-world monkeys, suggesting that there has been selection for the 42-bp unit length and repeat sequences in great apes and humans. Because telomere homeostasis is involved in many physiological and pathological processes, the diverse set of VNTR2-1 allelic variations might have helped human evolution and adaption in extremely diverse environments. They offer multifaceted and adaptable, rather than simple binary, telomerase regulation in different tissues and cell types. However, such diversities might also have affected disease susceptibilities and longevity in humans.

Ever since the identification of the *hTERT* gene over two decades ago (49, 50), studies of its transcriptional regulation have been focused on its proximal promoter. Recently, polymorphisms of the *hTERT* locus have been associated with a wide range of human diseases (51, 52). Genome-wide association studies identified a large number of SNPs at the *hTERT* locus that were associated with leukocyte telomere length and susceptibilities to a broad spectrum of age-related conditions including most types of cancers, cardiovascular diseases, pulmonary fibrosis, male infertility, and human longevity (53–56). These SNPs clustered in two regions of the *hTERT* locus (22, 57). Whereas region 1 coincided with the hTERT promoter, the regulatory elements associated with region 2 (introns 2 and 3) remained to be identified. Region 2 was represented by three widely studied SNPs, rs2853676, rs2853667, and rs2736100, which were 636, 1,988, and 2,666 bp downstream of VNTR2-1, respectively. Because of its proximity to these SNPs, polymorphic VNTR2-1 could be the regulatory element in region 2 involved in the development of cancer and other age-related diseases. Indeed, as shown in our study, the length of VNTR2-1 was associated with longevity in AAs (Fig. 6*E*).

In summary, we have identified VNTR2-1, a distal regulatory element for the *hTERT* gene that functions in hTERT transcription and telomere homeostasis. VNTR2-1 contained a large array of E-boxes and possibly other TF binding sites; these TF site clusters may provide a binding platform with its occupancy dependent upon local concentrations of various transcriptional activators, enabling both a robust activation and a fine-tuned regulation of the *hTERT* gene. This VNTR2-1 element is likely a part of a telomerase-regulatory network that has been missing in previous studies. The presence of polymorphic VNTR2-1 alleles among human populations provides a molecular and genetic basis for the diversities of telomere homeostasis in humans and, consequently, for susceptibilities to a broad spectrum of human diseases.

Materials and Methods

BACs and Plasmids. BAC reporter H(wt) containing a 160-kb human-genomic DNA sequence that included the *hTERT* gene and two immediate neighboring loci was reported previously (27). Its derivative EboxDM, published previously (9), contained mutations at the upstream and downstream E-boxes (−165 nt and +43 nt relative to the transcription start site) of the hTERT promoter. Deletions within BAC constructs were performed via a two-step BAC recombineering method (58, 59). BAC reporters with partial VNTR2-1 deletion were constructed as shown in *SI Appendix*, Fig. S1. Retrovirus pBABE-hTERT was published previously (60), and all TF cDNAs were cloned into pLNCX (9).

Cell Culture and Transfection. NHF, mouse ESCs TC1, and Tel$^+$ and Tel$^-$ immortal human fibroblast lines 3C167b and GM847 cells were described previously. 3C167b3.1 (Tel$^+$), GM847.7 (Tel$^-$), and T2-5 cells were clones of 3C167b, GM847, and TC1 cells, respectively, and each contained a single chromosomal BAC acceptor site (26, 27). To study the regulation of the hTERT promoter in a chromatinized setting, single-copy BAC reporters were integrated into the BAC acceptor sites in these cells using the RMBT method (26, 27). All integrated BACs were validated by Southern blotting and sequencing of the junctions. Differentiation of mouse ESCs was described previously (36).

ChIP. ChIP experiments were performed using antibodies listed in *SI Appendix*, Table S1 as previously described (26). ENCODE ChIP-seq datasets were aligned against the hg38 reference genome. Because no sequence homologous to the 42-bp repeats was found outside of VNTR2-1 in the human genome, the sequence reads that were mapped to VNTR2-1 reflected actual TF binding to this genomic region.

CRISPR/Cas9-Mediated Gene Editing. sgRNA sequences were cloned into pSpCas9(BB)/GFP (61). MelJuSo and 293T cells were transfected with a pair of plasmids expressing sgRNA-targeting sequences CATCGAACGGCAGCTGCCTCACAC and GGCTCTCGCCTCCCGCGTGCC at two ends of VNTR2-1. Cells with top 10% green fluorescence were collected by fluorescence-activated cell sorting 48 h posttransfection, and single cells were plated into 96-well plates. Clones with VNTR2-1 deletions were identified by PCR analysis of genomic DNAs and validated by Southern blot analysis and sequencing deletion junctions.

Southern Blot Analysis of VNTR2-1. VNTR2-1 length and genomic deletion of VNTR2-1 were determined by Southern blot analyses. Probe MS contained 12 copies of the 42-bp sequence.

Gene-Expression Analyses. BAC DNAs/plasmids were transiently transfected into NHF and Tel$^+$ cells using Lipofectamine LTX (Thermo Fisher Scientific) for 48 h, and luciferase activities were determined using the Dual Luciferase Assay system (Promega). For BAC reporter assays, *Rluc* activity derived from the hTERT promoter was normalized to *Fluc* activity expressed from the constitutive CRR9 promoter. Similar results were obtained when *Rluc* activities were normalized to cell numbers as determined by thiazolyl blue tetrazolium bromide assays. qRT-PCR and luciferase assays were performed as previously described (37, 38). Levels of hTERT mRNA were normalized to 18S ribosomal RNA. All PCR and luciferase assays were performed in triplicate and repeated at least twice. Western analyses of TFs were performed as described previously (9).

Telomere Length and Telomerase Analyses. Telomere length and telomerase activity were measured by telomere restriction fragment analysis and telomerase repeat amplification protocol (TRAP) assays, respectively, as previously described (37, 38).

Xenograft Tumor Formation. Human MelJuSo cells (2×10^6) and derivatives at passage 25 (except for J1, passage 19) were trypsinized and mixed with Matrigel (BD Biosciences) in 100 μL volume and implanted subcutaneously into 6-wk-old nude mice (nu/nu) (Jackson Laboratory). Mice were monitored every other day until tumors appeared, and tumor volumes were measured with a caliper twice per week [$V = (L \times W \times W)/2$] until mice were killed either when tumors reached 1 cm^3 or on day 63. Tumors were fixed with 4% paraformaldehyde and subjected to histology examination or immunohistochemistry staining. GraphPad Prism 7 was used to generate Kaplan–Meier tumor-free survival and tumor-growth curves. All experiments were approved by the Institutional Animal Care and Use Committee in accordance with the *Guide for the Care and Use of Laboratory Animals* (62).

Sequencing Analysis of VNTR2-1. Genomic DNA panels of CAs and AAs were from the Georgia Centenarian Collection (the National Institute on Aging's Aging Cell Repository, Coriell Institute for Medical Research): CA control panel (n = 100), AA control panel (n = 78), and AA centenarian panel (n = 32). Centenarians were individuals from 98 to 108 y of age who were enrolled in the Georgia Centenarian Study, and control individuals were 20 to 59 y of age (39). The genomic DNA samples were derived from lymphoblastoid cell lines. One sample each in the AA and CA control panels was not recovered. VNTR2-1 sequences were determined using the PacBio SMRT sequencing method (40). VNTR2-1 sequences in each sample were PCR amplified using two pairs of nested primers (*SI Appendix*, Table S2). The internal primers were barcoded. VNTR2-1 fragments of similar sizes were pooled and sequenced at the Washington State University Genomics Core Laboratory. In each sequencing reaction, 64 barcoded PCR samples were pooled together and loaded onto SMRT cells for massive parallel sequencing. At least 150 circular consensus sequences (CCSs) were obtained from each barcoded sample, and two consensus sequences, one from each allele, were obtained by CCS alignment.

Statistical Analysis. A two-tailed Student's t test was used to compare relative gene expression and tumor growth. For the VNTR2-1 genotype–phenotype association analysis, subjects were stratified by VNTR2-1 repeat numbers (LL, LS or SS, L ≥76, S <76). To compare genotype frequencies in AA centenarian and AA control groups, a two-tailed χ^2 was performed to calculate the OR, the 95% CI of the OR, and the P value using GraphPad Prism version 6.00 (GraphPad Software). The datasets generated during the current study are available from the NIH Database of Genotypes and Phenotypes (dbGaP) on reasonable request.

Data Availability. Full VNTR2-1 sequences of CAs and AAs have been deposited in the NIH Database of Genotypes and Phenotypes. Individual-level data are available for download by authorized investigators: https://view.ncbi.nlm.nih.gov/dbgap-controlled. Data dictionaries and variable summaries are available on the dbGaP FTP site: https://ftp.ncbi.nlm.nih.gov/dbgap/studies/phs002428/phs002428.v1.p1. The public summary-level phenotype data may be browsed at the dbGaP study report page: https://www.ncbi.nlm.nih.gov/projects/gap/cgi-bin/study.cgi?study_id=phs002428.v1.p1. Please refer to the release notes for more details: https://ftp.ncbi.nlm.nih.gov/dbgap/studies/phs002428/phs002428.v1.p1/release_notes/Release_Notes.phs002428.hTERT_TandemRepeats.v1.p1.MULTI.pdf.

ACKNOWLEDGMENTS. This work was supported in part by NIH Grant R01GM071725 to J. Zhu, Team Science Award Grant 579152 from the Melanoma Research Alliance to J. Zhu, G.P.R., and S.G., and the Health Sciences and Services Authority of Spokane County. We thank Chloe A. Dugger for technical assistance and Drs. Tianjie Pu and Boyang Wu for assistance with tumor histological analysis. We also thank the Program of Laboratory Animal Resources and the Histology Core of Washington State University (WSU) Spokane and the Genomics Core at WSU Pullman.

1. T. de Lange, Shelterin: The protein complex that shapes and safeguards human telomeres. *Genes Dev.* **19**, 2100–2110 (2005).
2. Y. S. Cong, W. E. Wright, J. W. Shay, Human telomerase and its regulation. *Microbiol. Mol. Biol. Rev.* **66**, 407–425 (2002).
3. Y. Huang, P. Liang, D. Liu, J. Huang, Z. Songyang, Telomere regulation in pluripotent stem cells. *Protein Cell* **5**, 194–202 (2014).
4. I. Horikawa *et al*., Differential cis-regulation of human versus mouse TERT gene expression in vivo: Identification of a human-specific repressive element. *Proc. Natl. Acad. Sci. U.S.A.* **102**, 18437–18442 (2005).
5. W. Jia *et al*., A BAC transgenic reporter recapitulates in vivo regulation of human telomerase reverse transcriptase in development and tumorigenesis. *FASEB J.* **25**, 979–989 (2011).
6. K. J. Wu *et al*., Direct activation of TERT transcription by c-MYC. *Nat. Genet.* **21**, 220–224 (1999).
7. B. S. Goueli, R. Janknecht, Regulation of telomerase reverse transcriptase gene activity by upstream stimulatory factor. *Oncogene* **22**, 8042–8047 (2003).
8. D. Xu, J. Dwyer, H. Li, W. Duan, J. P. Liu, Ets2 maintains hTERT gene expression and breast cancer cell proliferation by interacting with c-Myc. *J. Biol. Chem.* **283**, 23567–23580 (2008).
9. Y. Zhao, D. Cheng, S. Wang, J. Zhu, Dual roles of c-Myc in the regulation of hTERT gene. *Nucleic Acids Res.* **42**, 10385–10398 (2014).
10. S. Wang, J. Zhu, The hTERT gene is embedded in a nuclease-resistant chromatin domain. *J. Biol. Chem.* **279**, 55401–55410 (2004).

11. D. Cheng *et al*., Repression of telomerase gene promoter requires human-specific genomic context and is mediated by multiple HDAC1-containing corepressor complexes. *FASEB J.* **31**, 1165–1178 (2017).
12. N. W. Kim *et al*., Specific association of human telomerase activity with immortal cells and cancer. *Science* **266**, 2011–2015 (1994).
13. J. W. Shay, S. Bacchetti, A survey of telomerase activity in human cancer. *Eur. J. Cancer* **33**, 787–791 (1997).
14. S. Horn *et al*., TERT promoter mutations in familial and sporadic melanoma. *Science* **339**, 959–961 (2013).
15. F. W. Huang *et al*., Highly recurrent TERT promoter mutations in human melanoma. *Science* **339**, 957–959 (2013).
16. B. Heidenreich, P. S. Rachakonda, K. Hemminki, R. Kumar, TERT promoter mutations in cancer development. *Curr. Opin. Genet. Dev.* **24**, 30–37 (2014).
17. K. Chiba *et al*., Cancer-associated TERT promoter mutations abrogate telomerase silencing. *eLife* **4**, e07918 (2015).
18. J. D. McKay *et al*.; EPIC Study, Lung cancer susceptibility locus at 5p15.33. *Nat. Genet.* **40**, 1404–1406 (2008).
19. M. T. Landi *et al*., A genome-wide association study of lung cancer identifies a region of chromosome 5p15 associated with risk for adenocarcinoma. *Am. J. Hum. Genet.* **85**, 679–691 (2009). Corrected in: *Am. J. Hum. Genet.* **88**, 861 (2011).
20. T. Rafnar *et al*., Sequence variants at the TERT-CLPTM1L locus associate with many cancer types. *Nat. Genet.* **41**, 221–227 (2009).
21. G. M. Petersen *et al*., A genome-wide association study identifies pancreatic cancer susceptibility loci on chromosomes 13q22.1, 1q32.1 and 5p15.33. *Nat. Genet.* **42**, 224–228 (2010).
22. S. E. Bojesen *et al*.; Australian Cancer Study; Australian Ovarian Cancer Study; Kathleen Cuningham Foundation Consortium for Research into Familial Breast Cancer (kConFab); Gene Environment Interaction and Breast Cancer (GENICA); Swedish Breast Cancer Study (SWE-BRCA); Hereditary Breast and Ovarian Cancer Research Group Netherlands (HEBON); Epidemiological study of BRCA1 & BRCA2 Mutation Carriers (EMBRACE); Genetic Modifiers of Cancer Risk in BRCA1/2 Mutation Carriers (GEMO), Multiple independent variants at the TERT locus are associated with telomere length and risks of breast and ovarian cancer. *Nat. Genet.* **45**, 371–384, 384e1–2 (2013).
23. Z. Wang *et al*., Imputation and subset-based association analysis across different cancer types identifies multiple independent risk loci in the TERT-CLPTM1L region on chromosome 5p15.33. *Hum. Mol. Genet.* **23**, 6616–6633 (2014).
24. S. Wang, Y. Zhao, C. Hu, J. Zhu, Differential repression of human and mouse TERT genes during cell differentiation. *Nucleic Acids Res.* **37**, 2618–2629 (2009).
25. F. Zhang, D. Cheng, S. Wang, J. Zhu, Human specific regulation of the telomerase reverse transcriptase gene. *Genes (Basel)* **7**, E30 (2016).
26. D. Cheng *et al*., Regulation of human and mouse telomerase genes by genomic contexts and transcription factors during embryonic stem cell differentiation. *Sci. Rep.* **7**, 16444 (2017).
27. S. Wang, Y. Zhao, M. A. Leiby, J. Zhu, Studying human telomerase gene transcription by a chromatinized reporter generated by recombinase-mediated targeting of a bacterial artificial chromosome. *Nucleic Acids Res.* **37**, e111 (2009).
28. S. Wang, G. P. Robertson, J. Zhu, A novel human homologue of Drosophila polycomblike gene is up-regulated in multiple cancers. *Gene* **343**, 69–78 (2004).
29. H. Szutorisz *et al*., Rearrangements of minisatellites in the human telomerase reverse transcriptase gene are not correlated with its expression in colon carcinomas. *Oncogene* **20**, 2600–2605 (2001).
30. W. Kim *et al*., Regulation of the human telomerase gene TERT by telomere position effect-over long distances (TPE-OLD): Implications for aging and cancer. *PLoS Biol.* **14**, e2000016 (2016).
31. A. C. Bell, A. G. West, G. Felsenfeld, The protein CTCF is required for the enhancer blocking activity of vertebrate insulators. *Cell* **98**, 387–396 (1999).
32. A. Sabò, B. Amati, Genome recognition by MYC. *Cold Spring Harb. Perspect. Med.* **4**, a014191 (2014).
33. S. Wang, J. Zhu, Evidence for a relief of repression mechanism for activation of the human telomerase reverse transcriptase promoter. *J. Biol. Chem.* **278**, 18842–18850 (2003).
34. J. H. Chai *et al*., Regulation of hTERT by BCR-ABL at multiple levels in K562 cells. *BMC Cancer* **11**, 512 (2011).
35. D. Xu *et al*., Switch from Myc/Max to Mad1/Max binding and decrease in histone acetylation at the telomerase reverse transcriptase promoter during differentiation of HL60 cells. *Proc. Natl. Acad. Sci. U.S.A.* **98**, 3826–3831 (2001).
36. S. Wang, C. Hu, J. Zhu, Transcriptional silencing of a novel hTERT reporter locus during in vitro differentiation of mouse embryonic stem cells. *Mol. Biol. Cell* **18**, 669–677 (2007).
37. R. Mathew *et al*., Robust activation of the human but not mouse telomerase gene during the induction of pluripotency. *FASEB J.* **24**, 2702–2715 (2010).
38. D. Cheng *et al*., Engineering a humanized telomerase reverse transcriptase gene in mouse embryonic stem cells. *Sci. Rep.* **9**, 9683 (2019).
39. L. W. Poon *et al*., The Georgia centenarian study. *Int. J. Aging Hum. Dev.* **34**, 1–17 (1992).
40. X. Guo *et al*., SMRT sequencing for parallel analysis of multiple targets and accurate SNP phasing. *G3 (Bethesda)* **5**, 2801–2808 (2015).
41. J. Campisi *et al*., From discoveries in ageing research to therapeutics for healthy ageing. *Nature* **571**, 183–192 (2019).
42. S. H. Leem *et al*., The human telomerase gene: Complete genomic sequence and analysis of tandem repeat polymorphisms in intronic regions. *Oncogene* **21**, 769–777 (2002).
43. N. D. Heintzman *et al*., Distinct and predictive chromatin signatures of transcriptional promoters and enhancers in the human genome. *Nat. Genet.* **39**, 311–318 (2007).
44. H. K. Long, S. L. Prescott, J. Wysocka, Ever-changing landscapes: Transcriptional enhancers in development and evolution. *Cell* **167**, 1170–1187 (2016).
45. R. Gemayel, M. D. Vinces, M. Legendre, K. J. Verstrepen, Variable tandem repeats accelerate evolution of coding and regulatory sequences. *Annu. Rev. Genet.* **44**, 445–477 (2010).
46. R. V. Espley *et al*., Multiple repeats of a promoter segment causes transcription factor autoregulation in red apples. *Plant Cell* **21**, 168–183 (2009).
47. C. Balestrieri *et al*., Co-optation of tandem DNA repeats for the maintenance of mesenchymal identity. *Cell* **173**, 1150–1164.e14 (2018).
48. O. Ecevit, M. A. Khan, D. J. Goss, Kinetic analysis of the interaction of b/HLH/Z transcription factors Myc, Max, and Mad with cognate DNA. *Biochemistry* **49**, 2627–2635 (2010).
49. T. M. Nakamura *et al*., Telomerase catalytic subunit homologs from fission yeast and human. *Science* **277**, 955–959 (1997).
50. M. Meyerson *et al*., hEST2, the putative human telomerase catalytic subunit gene, is up-regulated in tumor cells and during immortalization. *Cell* **90**, 785–795 (1997).
51. E. H. Blackburn, E. S. Epel, J. Lin, Human telomere biology: A contributory and interactive factor in aging, disease risks, and protection. *Science* **350**, 1193–1198 (2015).
52. S. Mocellin *et al*., Telomerase reverse transcriptase locus polymorphisms and cancer risk: A field synopsis and meta-analysis. *J. Natl. Cancer Inst.* **104**, 840–854 (2012).
53. A. N. Burnett-Hartman *et al*., Telomere-associated polymorphisms correlate with cardiovascular disease mortality in Caucasian women: The cardiovascular health study. *Mech. Ageing Dev.* **133**, 275–281 (2012).
54. T. Mushiroda *et al*.; Pirfenidone Clinical Study Group, A genome-wide association study identifies an association of a common variant in TERT with susceptibility to idiopathic pulmonary fibrosis. *J. Med. Genet.* **45**, 654–656 (2008).
55. L. Yan, S. Wu, S. Zhang, G. Ji, A. Gu, Genetic variants in telomerase reverse transcriptase (TERT) and telomerase-associated protein 1 (TEP1) and the risk of male infertility. *Gene* **534**, 139–143 (2014).
56. D. Scarabino, M. Peconi, F. Pelliccia, R. M. Corbo, Analysis of the association between *TERC* and *TERT* genetic variation and leukocyte telomere length and human lifespan-A follow-up study. *Genes (Basel)* **10**, E82 (2019).
57. Z. Kote-Jarai *et al*.; COGS-CRUK GWAS-ELLIPSE (Part of GAME-ON) Initiative; UK Genetic Prostate Cancer Study Collaborators/British Association of Urological Surgeons' Section of Oncology; UK ProtecT Study Collaborators; PRACTICAL Consortium, Fine-mapping identifies multiple prostate cancer risk loci at 5p15, one of which associates with TERT expression. *Hum. Mol. Genet.* **22**, 2520–2528 (2013). Corrected in: *Hum. Mol. Genet.* **22**, 4239 (2013).
58. S. Wang, Y. Zhao, M. Leiby, J. Zhu, A new positive/negative selection scheme for precise BAC recombineering. *Mol. Biotechnol.* **42**, 110–116 (2009).
59. Y. Zhao, S. Wang, J. Zhu, A multi-step strategy for BAC recombineering of large DNA fragments. *Int. J. Biochem. Mol. Biol.* **2**, 199–206 (2011).
60. J. Zhu, H. Wang, J. M. Bishop, E. H. Blackburn, Telomerase extends the lifespan of virus-transformed human cells without net telomere lengthening. *Proc. Natl. Acad. Sci. U.S.A.* **96**, 3723–3728 (1999).
61. F. A. Ran *et al*., Genome engineering using the CRISPR-Cas9 system. *Nat. Protoc.* **8**, 2281–2308 (2013).
62. National Research Council, *Guide for the Care and Use of Laboratory Animals* (National Academies Press, Washington, DC, ed. 8, 2011).
63. ENCODE Project Consortium, An integrated encyclopedia of DNA elements in the human genome. *Nature* **489**, 57–74 (2012).